

# Magnetic Structure of Rare-Earth Nickel Boride-Carbides

V. A. Kalatsky

Department of Physics, Texas A&M University, College Station, Texas 77843-4242

V. L. Pokrovsky

Department of Physics, Texas A&M University, College Station, Texas 77843-4242  
and Landau Institute for Theoretical Physics, Kosygin str.2, Moscow 117940, Russia

(November 28, 1995)

We present a theory of the magnetic rare-earth nickel boride-carbides ( $\text{RENi}_2\text{B}_2\text{C}$ ,  $\text{RE}=\text{Ho, Er, Tm}$ ). Large total angular momentum allows one to employ semiclassical approximation and reduce the problem to the four-positional clock model. The latter gives a proper phase diagram in magnetic field-magnetic moment plane for varying directions of in-plane magnetic field. The theory explains recent experimental observations.

PACS numbers 74.72.Ny, 75.30.Cr, 75.30.Kz, 75.10.Dg

A complex phase diagram of  $\text{HoNi}_2\text{B}_2\text{C}$  in the temperature-magnetic field plane has been discovered in the neutron scattering experiments [1] and in measurements of resistivity [2]. Recent measurements of the anisotropic magnetization of  $\text{HoNi}_2\text{B}_2\text{C}$  by P. Canfield and coworkers [3,4] revealed a complicated magnetization-magnetic field diagram: re-entrant behavior for the low fields and a set of magnetic transitions for the high fields. The magnetic moment is highly anisotropic and has a strong dependence upon direction of magnetic field in the basal  $a$ - $b$  plane. A purpose of this article is to present a simple model for the magnetic subsystem in  $\text{RENi}_2\text{B}_2\text{C}$ , explaining the experimental facts.

The crystal structure of the  $\text{RENi}_2\text{B}_2\text{C}$  has been studied by T. Siegrist *et al.* [5] ( $\text{RE}=\text{Lu}$ ) and Q. Huang *et al.* [6] ( $\text{RE}=\text{Ho}$ ). The  $\text{RENi}_2\text{B}_2\text{C}$  compounds have the body-centered-tetragonal (bct) structure (space group  $I4/mmm$ ). A simplest form of the single-ion Hamiltonian compatible with the crystal field symmetry is

$$\mathcal{H}_{CEF} = \frac{a}{2}J_z^2 + \frac{b}{2}(J_+^4 + J_-^4), \quad (1)$$

where  $J_\pm$ ,  $J_z$  are components of the total angular momentum,  $a$  and  $b$  are crystal field constants. We assume that moments are presumably aligned in the  $a$ - $b$  plane and neglect terms proportional to  $J_z^4$  in comparison to those with  $J_z^2$ . The constant  $a$  must be positive to fix  $\mathbf{J}$  in the  $a$ - $b$  plane.

The fourth-order terms in Eq. (1) lift the  $O(2)$  degeneracy in favor of the four-fold symmetry. The Hamiltonian (1) can be treated quasi-classically since  $J_x$  and  $J_y$  are rather large ( $J=8, 15/2$ , and  $6$  for Ho, Er, and Tm, respectively). We introduce the angle  $\phi$  for the orientation of the moment  $\mathbf{J}$  in the  $a$ - $b$  plane, so that  $J_x = J \cos \phi$

and  $J_y = J \sin \phi$ . Then Hamiltonian (1) can be presented in the form

$$\mathcal{H} = -\frac{a}{2}\frac{\partial^2}{\partial\phi^2} + bJ^4(1 + \cos(4\phi)) - h \cos(\phi - \phi_h), \quad (2)$$

where  $h$  is the absolute value of the external magnetic field multiplied by  $5J\mu_B/4$ ,  $\phi_h$  is the angle between direction of magnetic field and reference tetragonal axis (*e.g.*  $a$  axis). Exploiting again a large value of  $J$ , it is natural to assume that  $2bJ^4 \gg a$ . Then the potential energy in (2) has deep wells at directions  $\phi = \pm\pi/4, \pm3\pi/4$ . Non-zero magnetic field destroys the tetragonal symmetry, but the symmetry breaking is small unless  $h$  exceeds the value  $bJ^4$  corresponding to fields essentially large than 20 T [7]. Thus, initially continuous moment  $\mathbf{J}$  is reduced to a discrete variable taking only four values. This is a kind of so-called clock model with 4 positions of the ‘‘hand’’.

Let us denote 4 states of the ‘‘hand’’ as  $|k\rangle$ , where  $k = 0, \dots, 3$ . Then the Hamiltonian (2) is equivalent to  $4 \times 4$  matrix

$$\hat{\mathcal{H}}_{kk'} = \epsilon_k \delta_{kk'} + w(\delta_{k,k'-1} + \delta_{k,k'+1}), \quad (3)$$

where  $\epsilon_k = -h \cos((2k+1)\pi/4 - \phi_h)$  and  $w$  is a matrix element of the ‘‘kinetic energy’’  $\frac{a}{2}\frac{\partial^2}{\partial\phi^2}$  between adjacent states of the ‘‘hand’’. In the approximation  $h \ll bJ^4$  all the overlap integrals are the same ( $w$ ). The diagonalization of the matrix (3) can be performed explicitly at any values of the parameters  $h$ ,  $\phi_h$ , and  $w$ . The lowest eigenvalue gives the energy of the ground state

$$E = -\sqrt{\frac{1}{2}\left(4w^2 + h^2 + \sqrt{(4w^2 + h^2)^2 - h^4 \cos(2\phi_h)^2}\right)}. \quad (4)$$

The result (4) explains the orientation dependent saturation in high magnetic field [3,4] (see Fig. 1). Namely, it has been observed in [4] that the magnetization along magnetic field reaches saturation values depending on direction according to the law  $M_s(\phi_h) \propto \cos(\pi/4 - \phi_h)$ . The moments in such a state are directed along an easy direction closest to the direction of the field. The direction-dependent saturation Fig. 1 is an intermediate asymptotic corresponding to the field interval  $w \ll h \ll bJ^4$ . At higher fields  $h \gg bJ^4$  the direction independent saturation is reached.

Further we employ this simplified description of the localized moments with minor modification to incorporate the collective effects. Let us introduce variables  $k_r = 0, \dots, 3$  at each site of the lattice and the interaction Hamiltonian

$$\mathcal{H}_i = \sum_{\mathbf{r}, \mathbf{r}'} K_{\mathbf{r}, \mathbf{r}'} \cos \frac{\pi}{2} (k_{\mathbf{r}} - k_{\mathbf{r}'}) + \sum_{\mathbf{r}, \mathbf{r}'} L_{\mathbf{r}, \mathbf{r}'} \cos \pi (k_{\mathbf{r}} - k_{\mathbf{r}'}), \quad (5)$$

where  $K_{\mathbf{r}, \mathbf{r}'}$  and  $L_{\mathbf{r}, \mathbf{r}'}$  are interaction energies. Only nearest neighbor interaction will be taken into account, so that the only non-zero constants are  $K_{\mathbf{r}, \mathbf{r} \pm \mathbf{a}} = K_{\mathbf{r}, \mathbf{r} \pm \mathbf{b}} = -\frac{1}{2} K_{\parallel}$ ,  $L_{\mathbf{r}, \mathbf{r} \pm \mathbf{a}} = L_{\mathbf{r}, \mathbf{r} \pm \mathbf{b}} = -\frac{1}{2} L_{\parallel}$ ,  $K_{\mathbf{r}, \mathbf{r} \pm \mathbf{c}/2} = K_{\perp}$  and  $L_{\mathbf{r}, \mathbf{r} \pm \mathbf{c}/2} = L_{\perp}$ , where  $\mathbf{a}, \mathbf{b}, \mathbf{c}$  are the primitive vectors of the lattice. We assume that  $K_{\parallel} > K_{\perp} > 0$ ,  $|L_{\parallel}| > |L_{\perp}|$ . For simplification we put ( $L_{\parallel} = L_{\perp} = 0$ ).

In this article we find only the ground state of the total Hamiltonian  $\mathcal{H} = \mathcal{H}_s + \mathcal{H}_i$  where the single-ion Hamiltonian  $\mathcal{H}_s$  is the direct sum of matrices (3). The ground state will be supposed to be homogeneous in-plane. The existing experimental data have no agreement upon the in plane structure of  $\text{HoNi}_2\text{B}_2\text{C}$ . The experiments performed on single crystals by Goldman, *at al.* [1], have clear presence of the satellites at  $0.585\mathbf{a}^*$  in the temperature range of 5–6 K. On the other hand neutron powder diffraction measurements by Grigereit, *at al.* [8,6], did not find evidence of these satellites. Both groups agree that the structure in the  $a$ - $b$  plane transits to the ferromagnetically aligned sheets below 5 K. We will assume ferromagnetic ordering in the  $a$ - $b$  plane. This implies that  $K_{\parallel} > 0$ . The antiferromagnetic order in  $c$ -direction implies that  $K_{\perp} > 0$ .

We apply a variational procedure, assuming the total wave function to be a product of single-ion wave functions. The wave functions at sites belonging to the same  $a$ - $b$  plane are assumed to be identical. Neighboring planes are assumed to belong to different sublattices 1 and 2. The single-ion states are described by two set of variational parameters  $\alpha_k, \beta_k$ ,  $k = 0, \dots, 3$  where  $\alpha_k$  and  $\beta_k$  are the amplitudes for a “hand” to be in the  $k$ 'th potential well for the first and second sublattice respectively. With this premises the energy per site is

$$\begin{aligned} \mathcal{H}_{var} = & \frac{K_{\perp}}{2} [(\alpha_0^2 - \alpha_2^2)(\beta_0^2 - \beta_2^2) + (\alpha_1^2 - \alpha_3^2)(\beta_1^2 - \beta_3^2)] \\ & - \frac{K_{\parallel}}{4} [(\alpha_0^2 - \alpha_2^2)^2 + (\alpha_1^2 - \alpha_3^2)^2 + (\beta_0^2 - \beta_2^2)^2 + (\beta_1^2 - \beta_3^2)^2] \\ & + w[(\alpha_0 + \alpha_2)(\alpha_1 + \alpha_3) + (\beta_0 + \beta_2)(\beta_1 + \beta_3)] \\ & - \frac{h_x}{2} [(\alpha_0^2 - \alpha_2^2) + (\beta_0^2 - \beta_2^2)] \\ & - \frac{h_y}{2} [(\alpha_1^2 - \alpha_3^2) + (\beta_1^2 - \beta_3^2)]. \end{aligned} \quad (6)$$

where  $h_x = h \cos(\pi/4 - \phi_h)$  and  $h_y = h \sin(\pi/4 - \phi_h)$ , due to the symmetry the consideration is constricted to

the range  $0 \leq \phi_h \leq \pi/4$ . The minimization of the Hamiltonian (6) with the constraints  $\sum \alpha_i^2 = \sum \beta_i^2 = 1$  leads to a system of nonlinear equations which allows a partial separation of variables. Proper variables are determined by following relations

$$\begin{aligned} \cos \zeta_1 &= \alpha_0^2 - \alpha_1^2 - \alpha_2^2 + \alpha_3^2, \\ \cos \zeta_2 &= \beta_0^2 - \beta_1^2 - \beta_2^2 + \beta_3^2, \\ \cos \eta_1 &= \alpha_0^2 + \alpha_1^2 - \alpha_2^2 - \alpha_3^2, \\ \cos \eta_2 &= \beta_0^2 + \beta_1^2 - \beta_2^2 - \beta_3^2. \end{aligned} \quad (7)$$

In terms of  $\zeta_i$  and  $\eta_i$  the minimization conditions read as follows

$$\begin{aligned} K_{\perp} \cos \zeta_1 - K_{\parallel} \cos \zeta_2 - 2 \cot \zeta_2 &= h_x - h_y, \\ K_{\perp} \cos \zeta_2 - K_{\parallel} \cos \zeta_1 - 2 \cot \zeta_1 &= h_x - h_y, \\ K_{\perp} \cos \eta_1 - K_{\parallel} \cos \eta_2 - 2 \cot \eta_2 &= h_x + h_y, \\ K_{\perp} \cos \eta_2 - K_{\parallel} \cos \eta_1 - 2 \cot \eta_1 &= h_x + h_y, \end{aligned} \quad (8)$$

where  $w$  has been set to 1. The systems of equations (8) have been solved numerically.

In the general case  $0 < \phi_h < \pi/4$  there are three phases and two first order phase transitions at fields  $h_{c1}(\phi_h)$  and  $h_{c2}(\phi_h)$ . In the range of small magnetic field the most energy favorable is antiferromagnetic phase (AF), in which spins in one sublattice are parallel whereas spins of the neighboring sublattices are antiparallel. At increasing field it is replaced by the ferrimagnetic phase (FM), in which spins of the neighboring sublattices are perpendicular. Finally the spin-flip proceeds into a phase with almost parallel spins in the neighboring sublattices (paramagnetic or spin-flip phase (PM)). In special cases of  $\phi_h = 0$  and  $\phi_h = \pi/4$  the numbers of phases and phase transitions are reduced by one. Namely, for  $\phi_h = 0$  the system undergoes a transition from the AF into the FM, final paramagnetic saturation happens for experimentally unreachable magnetic field  $h > bJ^4$ . For  $\phi_h = \pi/4$  the system takes up from the AF directly into the PM. Numerically found diagram in  $h$ - $\phi_h$  plane is presented on Fig. 2 for  $K_{\perp} = 3$ ,  $K_{\parallel} = 4$ .

For the two phase transitions and magnetization discontinuities at the transition points we find

$$h_{c1} = \frac{h_c}{\cos \phi_h}, \quad h_{c2} = \frac{h_c}{\sin \phi_h}, \quad (9)$$

$$\Delta M_1 = M_c \cos \phi_h, \quad \Delta M_2 = M_c \sin \phi_h \quad (10)$$

where  $h_c = h_c(K_{\perp}, K_{\parallel})$  and  $M_c = M_c(K_{\perp}, K_{\parallel})$ . The graphs of  $h_c$  and  $M_c$  *vs.*  $K_{\parallel}$  for some particular values of  $K_{\perp}$  are given at Figs. 3 and 4, respectively. The graphs of magnetization *vs.* magnetic field for different direction of the field are shown in Fig. 5.

A series of simple relationships can be obtained in a limiting case of  $K_{\parallel} \gg w$ , well approaching the conditions of the experiments. Then the “hands” are tightly

bound to the tetragonal easy directions. Magnetic field lifts four-fold symmetry and one of the “hands” (labeled by  $\alpha_i$  for definiteness) is set to the easy direction closest to the direction of magnetic field  $\alpha_0^2 = 1$  and  $\alpha_i = 0$ ,  $i = 1, 2, 3$ . The other “hand” can take three positions ( $\beta_3 = 0$ ) depending upon strength and direction of magnetic field. The three positions correspond to the three phases, *i.e.*, AF  $\beta_2^2 = 1$ ,  $\beta_i = 0$ ,  $i = 0, 1$ , FM  $\beta_1^2 = 1$ ,  $\beta_i = 0$ ,  $i = 0, 2$ , and PM  $\beta_0^2 = 1$ ,  $\beta_i = 0$ ,  $i = 1, 2$ . The energies, magnetization and transition lines can be found straightforwardly resulting in

$$h_c(K_\perp, K_\parallel \rightarrow \infty) = \frac{K_\perp}{\sqrt{2}}, \quad M_c(K_\perp, K_\parallel \rightarrow \infty) = \frac{1}{\sqrt{2}}. \quad (11)$$

These facts are confirmed clearly by numerical analysis (see Figs. 3 and 4).

The results fit reasonably well the experimental facts. P. C. Canfield *et. al.* [4] have observed three phase transitions instead of two predicted by our theory. We denote the experimental lines as  $H_{c1}(\phi_h)$ ,  $H_{c2}(\phi_h)$ , and  $H_{c3}(\phi_h)$ . It has been found [4] that the dependencies are

$$H_{c1} = \frac{3.36\text{kG}}{\cos(\pi/4 - \phi_h)}, \quad H_{c3} = \frac{9\text{kG}}{\sin \phi_h}.$$

There has been no evaluation given for  $H_{c2}$ . Our critical lines  $h_{c1}$  and  $h_{c2}$  plausibly correspond to the experimental lines  $H_{c2}$  and  $H_{c3}$  respectively. There is a perfect fit between  $h_{c2}$  (see Eq. (9)) and  $H_{c3}$  giving  $h_c \approx 9\text{kG}$ . We have already noted the excellent agreement between the theory and experiment for the angular dependence of the saturation magnetization.

The drawback of the model is that one extra phase, observed in the experiment between lines  $H_{c1}$  and  $H_{c2}$ , is absent in our model. We presume that this is the chiral phase seen in the zero-field neutron diffraction experiments [8,1] (the satellite  $0.915c^*$ ). Of course the spiral period might change in the presence of magnetic field. The spiral phase cannot be principally obtained in the framework of the two sublattice model. The number of layers should be at least equal to the ratio of the spiral structure period to the spacing between nearest holmium layers. The physical reason for appearance of the long-periodic modulated phase can be either RKKY forces or quantum tunneling ( $w$ ) which becomes active when the main collective interaction  $K_\perp$  favoring antiferromagnetism is suppressed by the magnetic field. Independent estimates of the quantum parameter  $w$  [3] show that it is rather small ( $w \sim 2\text{--}2.5$  K). Nevertheless, it cannot be neglected since it determines the magnetic susceptibility in the low-temperature limit.

We have shown that a simple 4-position clock model stemming from the quasiclassical single-ion Hamiltonian explains the angular dependencies of the saturation magnetization and at least one of the transition points ob-

served in the experiment. We believe that this fact indicates convincingly that the 4-position model is valid for the magnetic subsystem of RE nickel boride-carbides.

Incorporating the simplest inter-spin interaction we have found two phase transitions between AF, FM and spin-flip phases. We expect that in a slightly modified model modulated phases are the ground-states in some range of parameters.

Among the predictions which can be checked experimentally we emphasize following ones:

- i) In FM phase the magnetization vectors of the sublattices are perpendicular each other.
- ii) The jumps of magnetization are simple functions of direction (see Eq. (10)).

Our next purpose is the thermodynamics of the model as well as consideration of the long period chiral structures.

We are grateful to P. C. Canfield and collaborators for the opportunity to read their articles [2,3] prior publication and especially to D. Naugle for numerous discussions.

- 
- [1] A. I. Goldman, C. Stassis, P. C. Canfield, J. Zaretsky, P. Dervenagas, B. K. Cho, D. C. Johnston, and B. Sternlieb, *Phys. Rev. B* **50**, 9668 (1994).
  - [2] K. D. D. Rathnayaka, D. G. Naugle, B. K. Cho, and P. C. Canfield, *Phys. Rev. B* in press.
  - [3] B. K. Cho, B. N. Harmon, D. C. Johnston, and P. C. Canfield, submitted to *Phys. Rev. B*.
  - [4] P. C. Canfield, private communications.
  - [5] T. Siegrist, H. W. Zandbergen, R. J. Cava, J. J. Krajewski, and W. F. Peck, Jr., *Nature* **367**, 254 (1994).
  - [6] Q. Huang, A. Santoro, T. E. Grigereit, J. W. Lynn, R. J. Cava, J. J. Krajewski, and W. F. Peck, Jr., *Phys. Rev. B* **51**, 3701 (1995).
  - [7] This fact follows from the measurements of saturated magnetization [4] which do not display any tendency to isotropisation at field  $H \sim 20$  T.
  - [8] T. E. Grigereit, J. W. Lynn, Q. Huang, A. Santoro, R. J. Cava, J. J. Krajewski, and W. E. Peck, Jr., *Phys. Rev. Lett.* **73**, 2756 (1994).

FIG. 1. Magnetization *vs.* magnetic field for magnetic field direction (from top to bottom)  $\phi_h = 45, 36, 27, 18, 9$ , and  $0$  degrees, respectively, the single-ion model (see Eqs. (3,4)).  $\phi_h = 0$  corresponds to the direction  $[100]$  and  $\phi_h = \pi/4$  to  $[110]$ .

FIG. 2.  $h$ - $\phi_h$  phase diagram,  $K_\perp = 3$ ,  $K_\parallel = 4$ , the two sublattice model.

FIG. 3.  $h_c$  (see Eq.(9)) *vs.*  $K_{\parallel}$ , for interplane interaction (from top to bottom)  $K_{\perp} = 3, 1.5, 0.5,$  and  $0.2,$  respectively, the two sublattice model.

FIG. 4.  $M_c$  (see Eq.(10)) *vs.*  $K_{\parallel}$ , the two sublattice model.

FIG. 5. Magnetization *vs.* magnetic field,  $K_{\perp} = 3,$   $K_{\parallel} = 4,$  the two sublattice model.

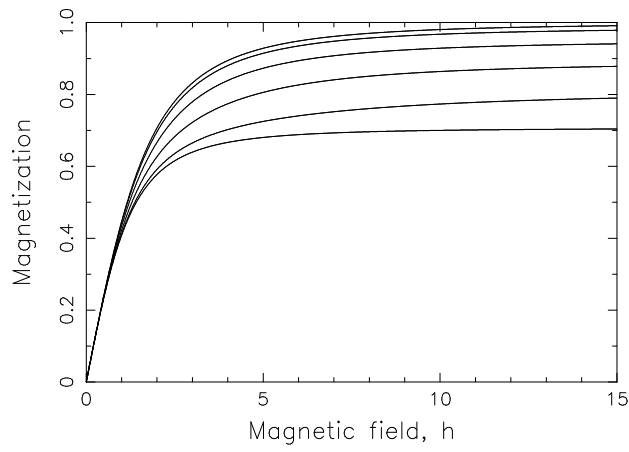


Fig.1

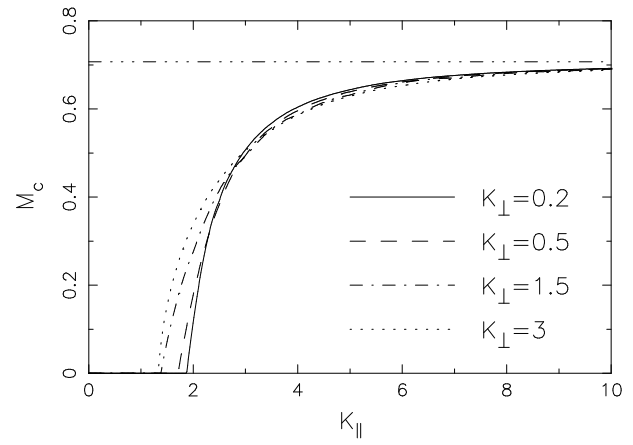


Fig.4

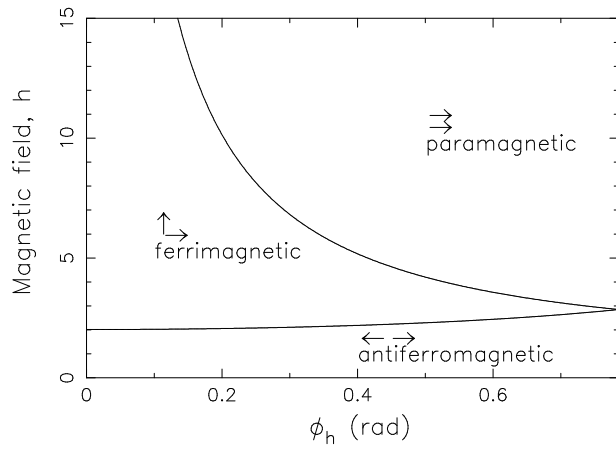


Fig.2

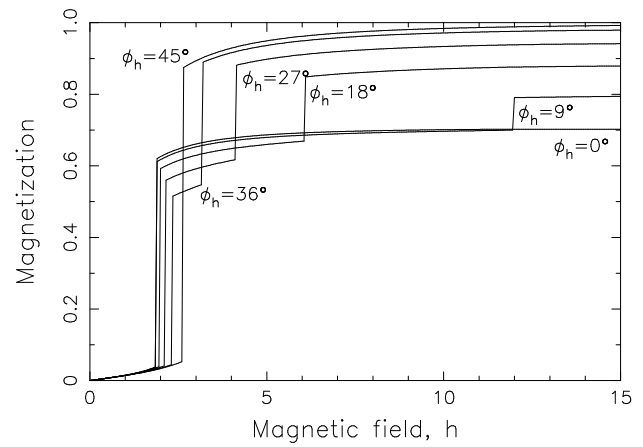


Fig.5

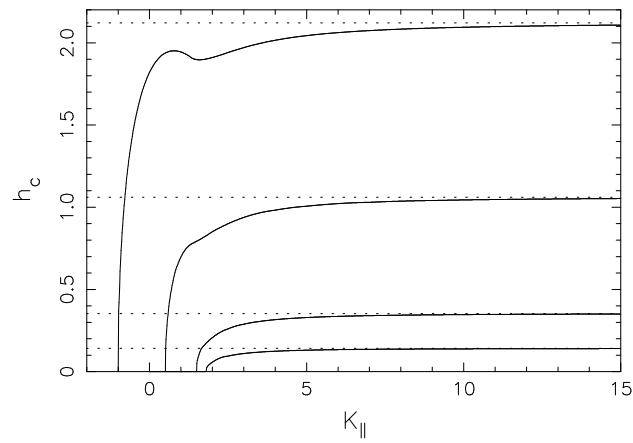


Fig.3